Three-Dimensional Optimization of Arterial Tree Models

R. Karch, W. Schreiner, M. Neumann, F. Neumann
Department of Medical Computer Sciences, Department of Cardiothoracic Surgery, Institute of Experimental Physics, University of Vienna, Spitalgasse 23, A-1090 Vienna, Austria
E-Mail: rudolf.karch@akh-wien.ac.at

Abstract

The computational method of Constrained Constructive Optimization has been generalized to grow arterial model trees within a three-dimensional perfusion volume, representing a piece of tissue to be supplied with blood. Starting from an inlet at the surface of the perfusion volume, a binary branching tree of cylindrical tubes is generated so as to fulfill several physiologic boundary conditions and constraints. The model tree is grown by successively adding terminal segments while optimizing the geometric location and topological site of each new connection according to minimum total intravasal volume. Introducing additional "post-optimization" steps into the optimization algorithm improves the degree of optimality (measured in terms of the target function) of the trees generated. While the structure of the resulting trees changes considerably, the pressure profile from inlet to terminals, representing a functional characteristic, remains practically unaffected.

1 Introduction

Computer models of arterial trees have frequently been used as the geometrical substrate for hemodynamic simulation studies. Until recently (cf. Neumann *et al.* [1]), these simulations were based either on compartmental representations or on branching tube models directly drawn from anatomical data or constructed as self-similar (stochastic) networks. In contrast to these models, the method of *Constrained Constructive Optimization* (CCO, Schreiner [2]) allows to generate in full detail (i.e., providing segment coordinates and diameters) "realistic" arterial model trees of some 10^4 vessel segments extending from the feeding artery down to the arteriolar level. Moreover, the CCO method is based on general optimality principles and does not rely on anatomical input data.

In previous implementations of the CCO method, the tree was grown in a two-dimensional perfusion volume according to given boundary conditions, a set of constraints, and an optimization target. Although two-dimensional CCO models were found to reproduce various anatomical and physiological properties of real arterial trees (including segment radii, branching angles, and pressure profiles) to a satisfying extent (Schreiner & Buxbaum [3]), these two-dimensional models clearly represent a conceptual simplification of reality. Therefore, our model has been extended to three dimensions to cover more realistic perfusion volumes and to overcome the restrictions inherent in the two-dimensional model. In the following we first present the algorithm used to grow three-dimensional CCO trees and then we discuss an extension of this algorithm towards improving the optimality of generated trees. Finally, we address the impact of this extension on structural and functional characteristics of CCO trees.

2 Methods

2.1 Basic model assumptions

Within the framework of CCO, the physiological characteristics of arterial trees are first mapped into a set of mathematical boundary conditions and constraints. The arterial tree is represented as a dichotomously branching network of rigid cylindrical tubes (*segments*), perfused at steady state conditions according to Poiseuille's law and subject to the following *physiological boundary conditions* and *constraints*:

- The pressures p_{term} at the distal ends of terminal segments are equal (and assumed to be the inflow pressures into the microcirculatory network, which is not modeled in detail).
- Each terminal segment i delivers an individual amount of blood flow $Q_{\text{term},i}$ against the constant pressure p_{term}.
- The laminar flow resistance of the whole tree induces a given total perfusion flow Q_{perf} along the overall pressure drop $\Delta p = p_{\text{perf}} - p_{\text{term}}$, where p_{perf} denotes the perfusion pressure in the feeding artery.
- N_{term} terminal segments (yielding $N_{\text{tot}} = 2N_{\text{term}} - 1$ segments in total) are distributed within the perfusion volume according to a predefined probability distribution.
- At bifurcations the radii of parent and daughter segments obey a power law (*bifurcation law*) of the form

$$r_{\text{parent}}^{\gamma} = r_{\text{left}}^{\gamma} + r_{\text{right}}^{\gamma} \tag{1}$$

with a constant exponent $\gamma > 0$. For the present work, the bifurcation exponent was set to $\gamma = 3$ (e.g., Sherman [4]).

It is a key requirement for the CCO method that all physiological boundary conditions and constraints regarding pressures, flows, and the bifurcation law, Eq. (1), can simultaneously be fulfilled by appropriate scaling of segment radii, regardless of the particular geometrical and topological (i.e., connective) structure of a given model tree (Schreiner & Buxbaum [3]).

2.2 Growing the tree

Starting from an inlet for the feeding artery at the surface of the perfusion volume, the model tree is grown by successively adding new terminal segments. A new terminal location $\mathbf{x}_{new}$ is drawn from a pseudo random number sequence with a given probability distribution. $\mathbf{x}_{new}$ is accepted only if both $\mathbf{x}_{new}$ is within the perfusion volume and the distance of $\mathbf{x}_{new}$ to all preexisting segments exceeds an adaptive threshold value (*distance criterion*). This new terminal site is then tentatively connected to a fixed number (N_{con}) of preexisting segments in the vicinity of $\mathbf{x}_{new}$ (*connection search*). Since the addition of a new terminal segment violates the boundary conditions and constraints for pressures and flows as well as the bifurcation law, Eq. (1), these must be reestablished for each temporary connection by proper rescaling of all segment radii according to Poiseuille's law for laminar flow resistance. For each connection $j = 1,\ldots,N_{con}$ a new bifurcation is generated, geometrically optimized (see below), and removed again. The results of each optimization step together with the diagnostics of geometry checks (e.g., segment intersections) are recorded in line j of a so-called *connection evaluation table* (CET) assigned to $\mathbf{x}_{new}$. In a last step, the CET is scanned for all possible (i.e., geometrically reasonable) connections, yielding a subset CET_r of the connection evaluation table; unless CET_r is the empty set (in which case the tossing for a new terminal location is repeated), the optimal connection in CET_r is adopted as permanent for the new terminal site $\mathbf{x}_{new}$. At this stage of tree development the locations of all bifurcations can optionally be reoptimized (post-optimization step, see below). The above procedure of successively adding new terminal segments is repeated until the preset maximum number of terminals is achieved, which in turn defines the "resolution" of the model tree.

Figure 1 shows a CCO-generated three-dimensional arterial tree with 2000 terminal segments (3999 segments in total) perfusing a spherical piece of model tissue with a radius of $r_{perf} = 3$ cm. The tree was generated with equal flows $Q_{term} = Q_{perf}/N_{term}$ for all terminal segments, a uniform probability distribution for their respective locations, and optimized for minimum total intravasal volume without performing the post-optimization steps. Perfusion pressure, terminal pressure, and perfusion flow were set to p_{perf} = 100 mmHg, p_{term} = 60 mmHg, and Q_{perf} = 500 ml/min, respectively.

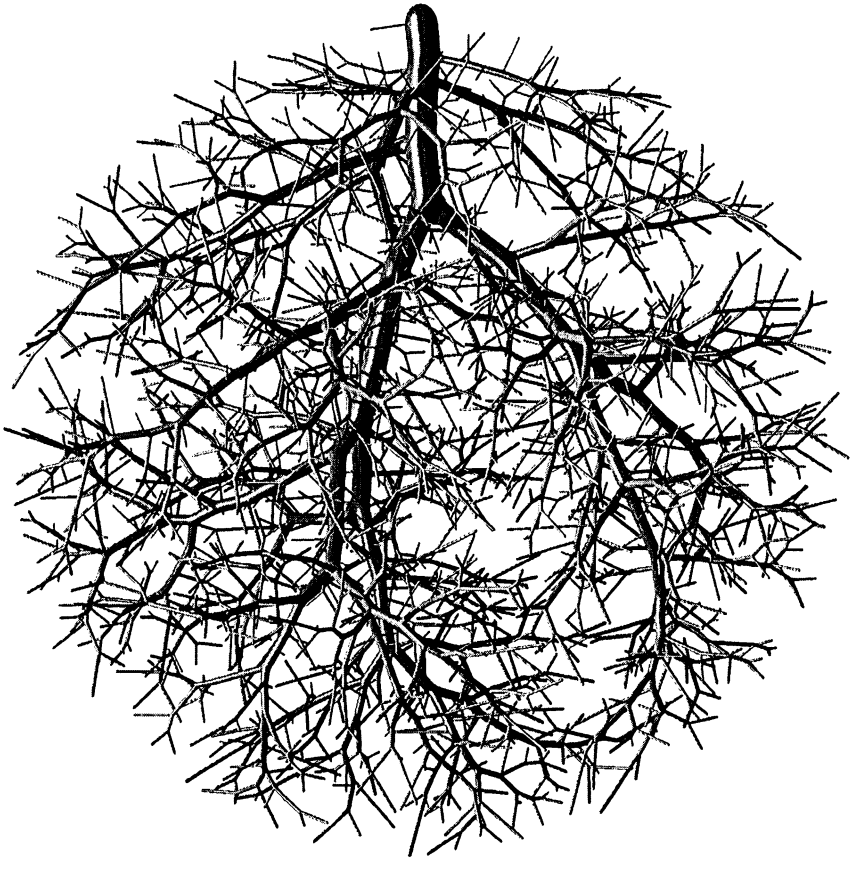

Figure 1: CCO-generated three-dimensional arterial model tree with 2000 terminal segments optimized for minimum intravasal volume without post-optimization. Visualization was performed by means of the isosurface algorithm for image-based direct volume rendering (Neumann *et al.* [5]).

2.3 Optimizing the tree

Arterial trees serve the purpose of efficiently carrying blood to all sites of tissue, representing a fluid transport system costly to construct and to maintain (LaBarbera [6]). Assuming that growth and structure of arterial trees are not purely arbitrary but governed by (global) optimality principles (Zamir [7]), the question arises which principles to adopt for a simulation model to be physiologically reasonable, yet manageable on medium-scale computer facilities.

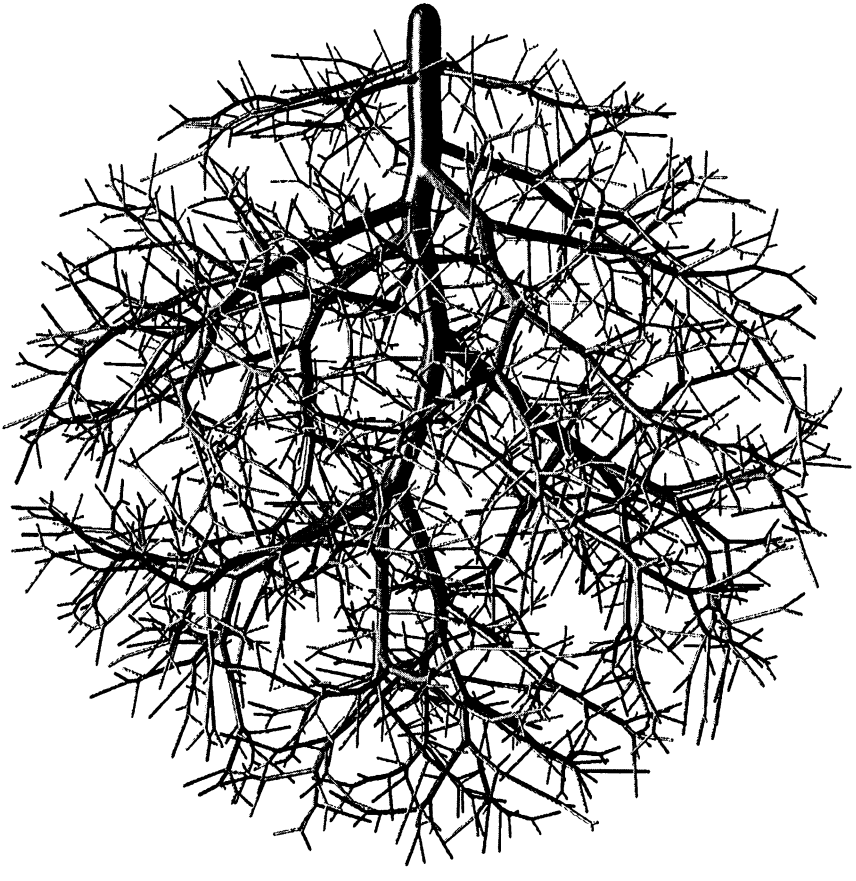

Figure 2: Three-dimensional arterial model tree with 2000 terminal segments generated by CCO with post-optimization performed. Simulation parameters were identical to those used for Figure 1.

To numerically characterize the degree of optimality of a given tree, a cost (or target) function (T) must be selected. Since the total intravasal volume (V) of the tree is a generally accepted choice for an optimization target function (Kamiya & Togawa [8]), T was set proportional to V for the present study,

$$T = \sum_{j=1}^{N_{\text{tot}}} l_j r_j^2 \,, \tag{2}$$

where l_j and r_j denote length and radius of segment j.

The CCO method comprises both local (geometric) and global (structural) aspects of optimization: When a new terminal site is tentatively connected to

an existing segment, the location of the resulting bifurcation is optimized (*geometric optimization*). After the connection search process, the connection corresponding to the minimum value of T is made permanent, which in turn defines the connective structure and hence the topology of the tree (*structural optimization*). Thus, minimizing T not only determines the geometric location of single bifurcations but also controls the global topological structure of the tree and both features are governed by the very same target function T.

Geometrically optimizing a single bifurcation requires to find a minimum of the target function T subject to a set of *optimization constraints* emerging from geometrical restrictions:

- The lengths of the three segments adjacent to the bifurcation being optimized must not degenerate.
- The bifurcation and—for a nonconvex geometry—all parts of the adjacent segments must remain within the perfusion volume.

Since the process of finding the minimum of T involves moving the bifurcation under consideration, the lengths of the 3 adjacent segments will generally change, thus violating the boundary conditions and constraints formulated in Section 2.2. Therefore, segment radii have to be simultaneously rescaled, which in turn changes T. The target function may be interpreted as a continuous function of all segment coordinates (Schreiner *et al.* [9]):

$$T = T(\{\mathbf{x}_i\}_{i=1,\ldots,N_{\text{tot}}}) \,. \tag{3}$$

On this basis, geometrical optimization under the above-mentioned constraints was implemented using a sequential quadratic programming algorithm [10].

Considering the generation of a new bifurcation by adding a terminal segment within the framework of global optimality, we notice that previously optimized bifurcations can no longer be optimal within the final tree due to the necessary changes of segment radii. This suggests the concept of *post-optimization*, which means to reoptimize the locations of all bifurcations in the tree after adding new terminal segments. In the following, we discuss the effect of post-optimization on the degree of optimality as well as on descriptors related to structure and functionality of the generated trees.

3 Results

Figure 2 illustrates a model tree generated with the same parameters that were used for Figure 1 but with post-optimization performed. The effect of this change in the optimization algorithm on tree structure is immediately evident to visual inspection by comparing the large mainstream segments in Figure 1 and Figure 2.

In order to characterize the changes due to post-optimization we first consider the question to what extent the *optimality* of the tree—measured in terms of the target function—will be improved if the whole tree is reoptimized each time a new terminal is added.

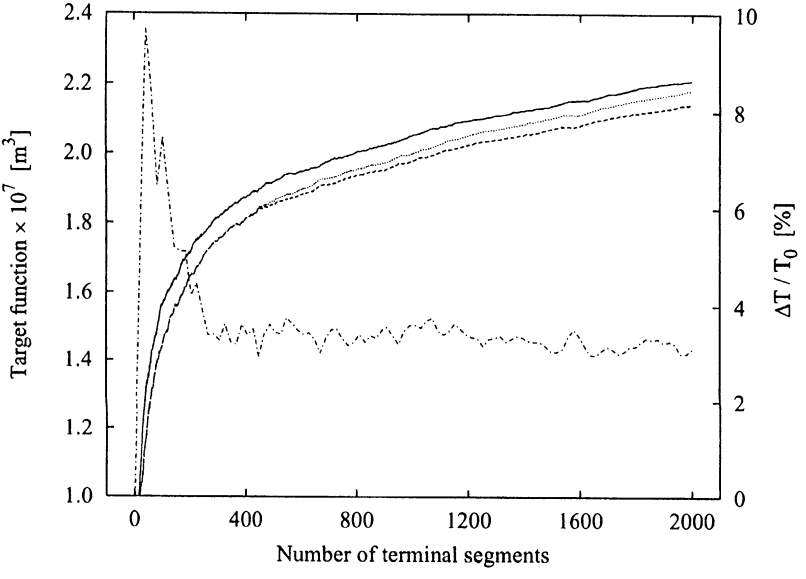

Figure 3: Target functions (left scale) during the growth of trees in Figure 1 (solid line) and Figure 2 (dashed line). The dotted line denotes partial post-optimization for the first 400 terminals. The dash-dotted line indicates the percentage decrease ΔT relative to its corresponding value T_0 without post-optimization (right scale).

Figure 3 demonstrates how the respective target functions evolve when the trees of Figure 1 and Figure 2 are grown from scratch. The curves show the behavior one would expect when the optimization algorithm is refined by additional post-optimization steps. On the expense of computational resource consumption, the overall decrease of the final target function value amounts to about 3% relative to its original value T_0 without post-optimization. The dash-dotted curve for the relative decrease $\Delta T/T_0$ of T demonstrates that post-optimization is most effective in the early stages of tree development. This is due to the large vessel segments being generated at the beginning of growth and because of sufficient space available to move them. As the number of terminals increases, $\Delta T/T_0$ decreases and remains almost constant during the course of growth, suggesting that the improvement of T can—to a large extent—be attributed to reoptimizing the first few hundred bifurcations at the beginning of tree generation. This observation is of considerable impact in the light of computational performance, since post-optimization renders CCO an $O(n^2)$ algorithm (and hence infeasible for large problems), whereas genuine CCO behaves like $O(n)$ due to the constant size of the neighborhood table employed for the connection search process (cf. Section 2.2): The dotted line in Figure 3 illustrates the gain in optimality when post-optimization was performed only during the addition of the first 400 terminals. Despite a run-time of approx. only 10%, the decrease ΔT of T was found to be about 50% of the value for full post-optimization.

Note, that $\Delta T/T_0$ is not a smooth function of N_{term}, since the topologies of the trees are different and actually diverge more and more as N_{term} increases (for the model trees in Figure 1 and Figure 2 the first transition to different connective structures was encountered after the trees were grown to only 10 segments).

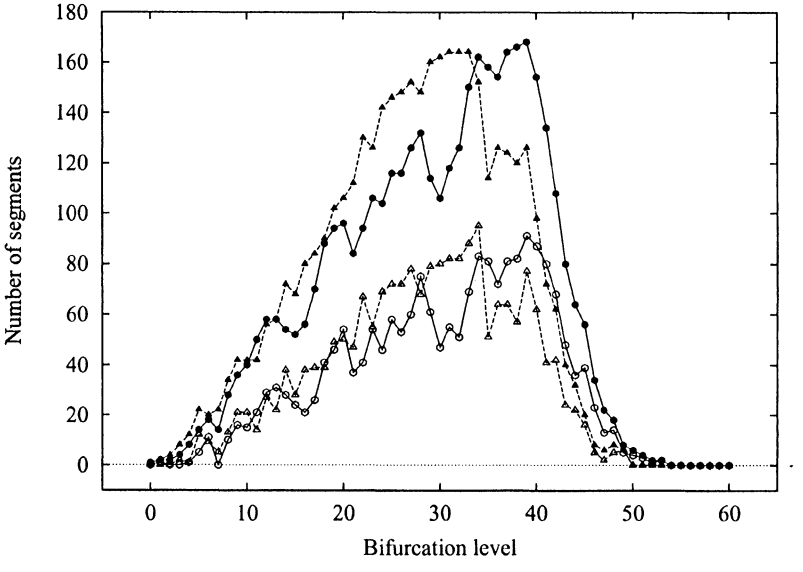

Figure 4: Frequency distribution of all segments (bulk symbols, upper curves) and of terminals only (open symbols, lower curves) over bifurcation levels found in the trees of Figure 1 (no post-optimization, solid lines) and Figure 2 (post-optimization, dashed lines).

To quantify the *structural* impact caused by post-optimization we consider the frequency distribution of segments over their bifurcation levels (Λ_{bif}), the latter being defined as the number of proximal bifurcations along the path from the respective segment towards the root segment. Post-optimization generally shifts the frequency distribution towards lower bifurcation levels (Figure 4); the respective modal values decrease by about 18% from level 39 to 32 (and by 13% from level 39 to 34 for the terminals). This means that the post-optimized tree branches more rapidly in proximal regions of the perfusion volume. Moreover, the highest bifurcation level of the post-optimized tree in Figure 2 ($\Lambda_{\text{bif}} = 49$) is by $\approx 8\%$ lower than that of the tree in Figure 1 ($\Lambda_{\text{bif}} = 53$). These findings correspond to the characteristics of "delivering" trees (Zamir [11], Schreiner *et al.* [9]) and CCO models optimized for hypervolume.

In order to assess the effects of post-optimization on the *functional* characteristics of the model trees, we evaluated their pressure profiles from the inlet to the terminal segments. Figure 5 demonstrates that pressure profiles remain almost unaffected by the structural changes induced by post-optimization, in accordance with previously reported results (cf. Schreiner *et al.* [12]).

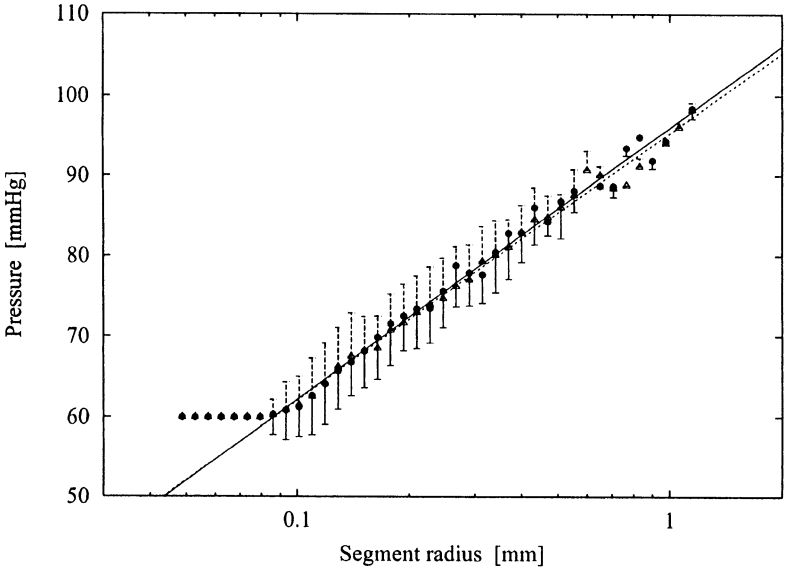

Figure 5: Pressure profiles for the reference trees of Figure 1 (no post-optimization, circles) and Figure 2 (post-optimization, triangles). Data-points indicate mean values over logarithmically equidistant segment radii-classes, bars denote standard deviations. Solid and dashed lines illustrate linear least-squares fits for the respective set of data-points (excluding terminal segments with $p_{\text{term}} = const$).

4 Conclusion

In the present paper we have demonstrated that our method of CCO can be generalized—from a previously two-dimensional implementation—to grow arterial model trees within a three-dimensional perfusion volume. Regarding global optimality of generated trees, partial post-optimization proved a practicable compromise between the degree of optimality and computational efficiency. Tree structures resulting thereof were found to be visually different and could be discriminated by means of their respective bifurcation levels. Functional features, characterized in terms of pressure profiles, remained unchanged.

References

1. Neumann, M., Neumann, F., Karch, R. & Schreiner, W. Spatially resolved simulation of coronary hemodynamics, in BIOSIM 96 (ed M. Cerrolaza, D. Jugo & C.A. Brebbia), pp. 39–51, *Proceedings of the 1st Int. Conf. on Simulation Modelling in Bioengineering*, Mérida, Venezuela, 1996, Computational Mechanics Publications, Southampton, 1996.

2. Schreiner, W. Computer generation of complex arterial tree models, *Journal of Biomedical Engineering*, 1993, **15**, 148–150.

3. Schreiner, W. & Buxbaum, P. Computer-optimization of vascular trees, *IEEE Transactions of Biomedical Engineering*, 1993, **40**, 482–491.

4. Sherman, T.F. On connecting large vessels to small: The meaning of Murray's law, *Journal of General Physiology*, 1981, **78**, 431–453.

5. Neumann, F., Neumann, M., Karch, R. & Schreiner, W. Visualization of computer-generated arterial model trees, in BIOSIM 96 (ed M. Cerrolaza, D. Jugo & C.A. Brebbia), pp. 259–268, *Proceedings of the 1st Int. Conf. on Simulation Modelling in Bioengineering*, Mérida, Venezuela, 1996, Computational Mechanics Publications, Southampton, 1996.

6. LaBarbera, M. Principles of design of fluid transport systems in zoology, *Science*, 1990, **249**, 992–999.

7. Zamir, M. Optimality principles in arterial branching, *Journal of Theoretical Biology*, 1976, **62**, 227–251.

8. Kamiya, A. & Togawa, T. Optimal branching structure of the vascular tree, *Bulletin of Mathematical Biophysics*, 1972, **34**, 431–438.

9. Schreiner, W., Neumann, F., Neumann, M., End, A. & Müller, M.R. Structural quantification and bifurcation symmetry in arterial tree models generated by constrained constructive optimization, *Journal of Theoretical Biology*, 1996, **180**, 161-174.

10. The Numerical Algorithms Group NAG Fortran Library Manual Mark 16, *The Numerical Algorithms Group Ltd*, Oxford, UK, 1993.

11. Zamir, M. Distributing and delivering vessels of the human heart, *Journal of General Physiology*, 1988, **91**, 725–735.

12. Schreiner, W., Neumann, F., Neumann, M., Karch, R., End, A. & Rödler, S.M. Limited bifurcation asymmetry in coronary arterial tree models generated by constrained constructive optimization, *Journal of General Physiology*, 1997, **109**, 1–12.